Electronic Supplementary Material (ESI) for Journal of Materials Chemistry A.
This journal is © The Royal Society of Chemistry 2020

Electronic Supplimentary Information for

Enhanced ion transport in an ether aided super concentrated ionic liquid electrolyte for long-life practical lithium metal battery applications

Urbi Pal, [a] Fangfang Chen, [a,b] Derick Gyabang, [a] Thushan Pathirana Senadhi, [a] Binayak Roy, [c] Robert Kerr,[a] Douglas R. MacFarlane, [b,c] Michel Armand, [a,d] Patrick C. Howlett, [a,b] Maria Forsyth * [a,b]

[a] Institute for Frontier Materials (IFM), Deakin University, Burwood, Victoria 3125, Australia.

[b] ARC Centre of Excellence for Electromaterials Science (ACES), Deakin University, Burwood, Victoria 3125, Australia.

[c] School of Chemistry, Monash University, Clayton 3800, Victoria, Australia.

[d] CIC EnergiGUNE, Parque Tecnológico de Álava, 48, 01510 Miñano, Álava, Spain.

Table S1: Modified VTF equation fitting parameters for different IL:DME electrolyte where the LiFSI salt concentration is 3.2 mol/kg

Modified VTF equation: $\sigma = \sigma o \exp(-\frac{\mathrm{Bo}}{(T-\mathrm{To})})$, where B_o =D* T_o

Composition	σ_o	B_o	T_o	D(=1/f)
100IL	0.48±0.09	780±17	174±8	4.46±0.04
90IL10DME	0.41±0.01	639±9	177±4	3.59±0.07
80IL20DME	0.44±0.07	601±19	177±2	3.38±0.03
70IL30DME	0.38±0.1	536±33	180±7	2.98±0.06
60IL40DME	0.41±0.09	503±15	178±3	2.81±0.04
50IL50DME	0.54±0.04	521±7	175±4	2.96±0.09

B_o is termed as the pseudo-activation energy and we can see that the pseudo activation energy for the electrolyte is decreasing with increasing DME percentage.

Table S2: Activation energy calculated from diffusion NMR and ionic conductivity for various IL:DME electrolytes; note the temperature range considered for this calculation is 10˚C to 60˚C with 10˚C intervals.

Arrhenius equation: $\ln k = \ln A - \frac{Ea}{RT}$

Composition	**Activation energy (Ea) using Arrhenius equation (kJ/mol)**				
	PFG NMR				Ionic conductivity (σ)
	^{1}H (C_3mpyr)	^{7}Li (Li^{+})	^{19}F (FSI^{-})	^{1}H (DME)	
100IL	29	37	34	-	35
90IL10DME	29	31	30	34	30
80IL20DME	31	31	30	33	28.5
70IL30DME	29	31	30	32	26
60IL40DME	30	31	30	33	24
50IL50DME	29	30	29	32	24

The activation energies of the species participating in the diffusion measurement (PFG-NMR) have been calculated by fitting the diffusion coefficient values using the Arrhenius equation and tabulated in table S2. The data show that the activation energy for FSI anion and lithium cation are decreasing when 10 wt% DME is added, and remains relatively constant thereafter. This shows that the DME is interacting with the FSI anion and Li cation, thereby affecting the transport mechanism and leading to a decrease in the activation energy. Interestingly, the C_3mpyr cation is unaffected by the DME addition which indicates that DME has lesser affinity towards the ionic liquid cation. In addition to this, the temperature dependent ionic conductivity data is also fitted using the Arrhenius equation under the same temperature range that we considered for PFG-NMR study (10°C to 60°C where it showed linear behaviour) and the activation energies are calculated and compared with those calculated for diffusion.

In table S2, it can be seen that the activation energy for the ionic conductivity is also decreased with increasing DME content which also supports the idea of DME facilitated ion transport through a continuous exchange in the coordination sphere of lithium.

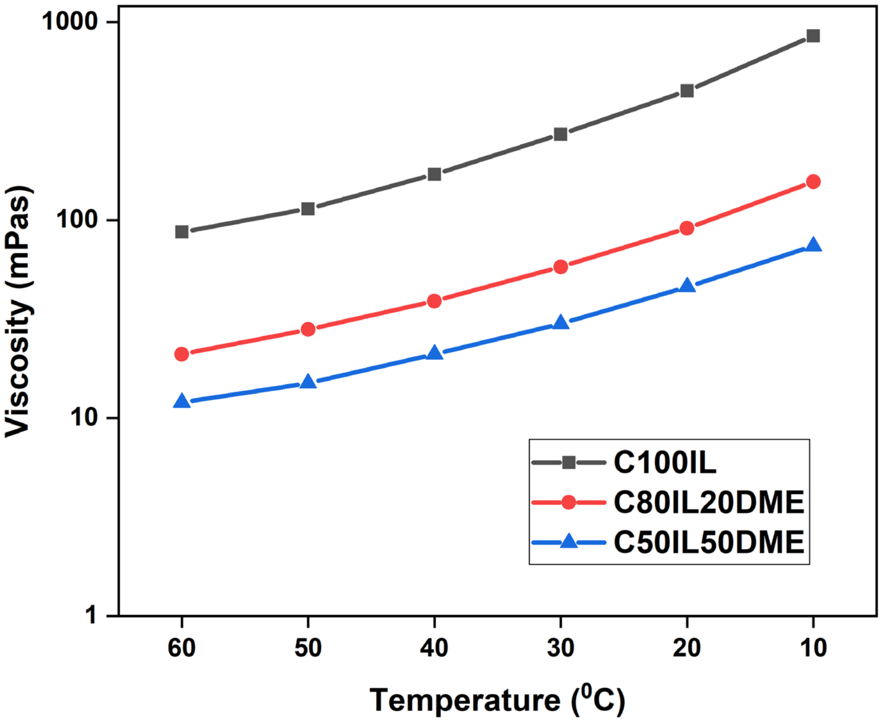

Figure S1: Temperature dependent viscosity of 100IL, 80IL20DME and 50IL50DME

The viscosity decreases significantly with increased amount of DME. In comparison to 100IL, the 50IL50DME shows almost 10 times lower viscosity in all the temperature ranges recorded in this experiment.

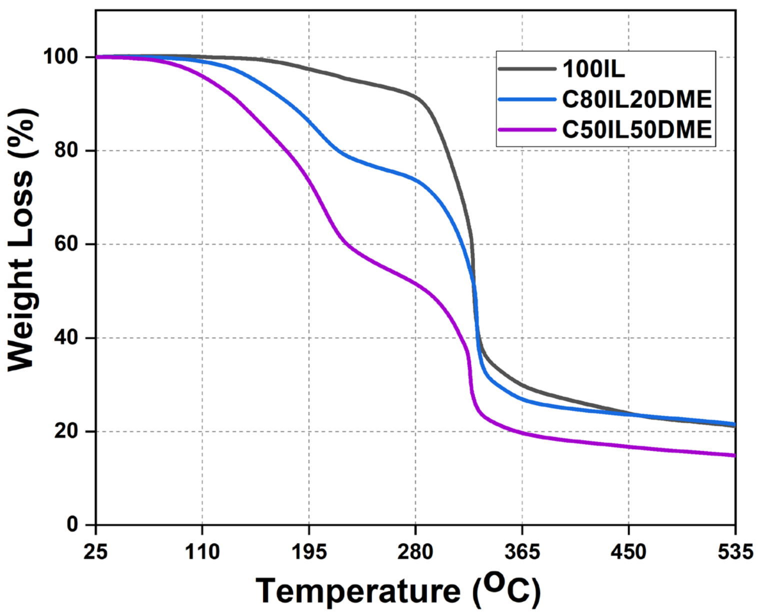

Figure S2: Thermo-gravimetric analysis (TGA) of 100IL, 80IL20DME and 50IL50DME

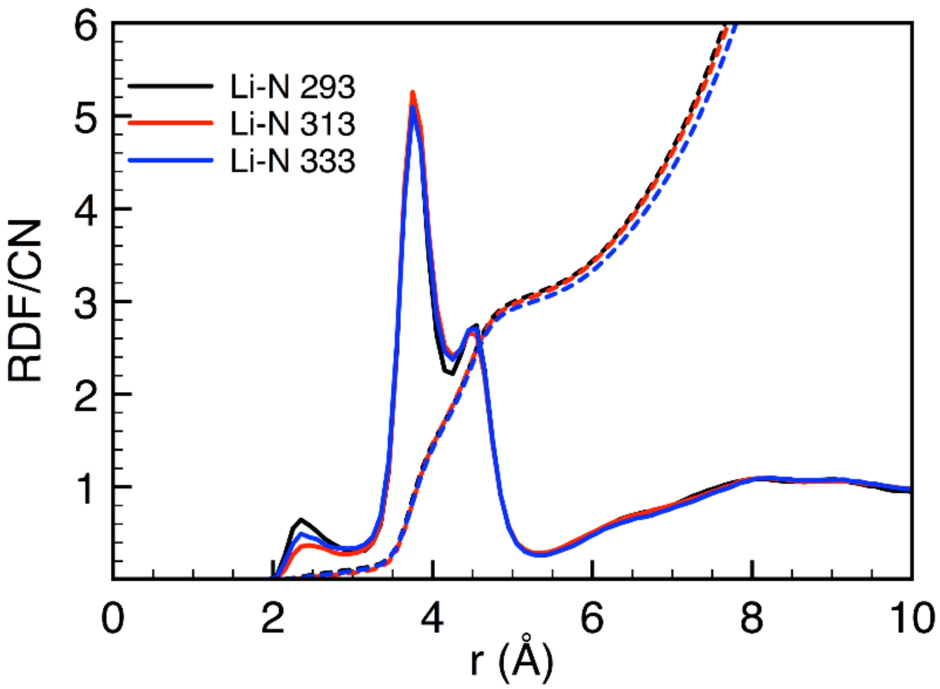

Figure S3: RDF of Li-N (FSI) at different temperatures of 293, 313 and 333 K

In this case, the diffusion of DME also affects Li^+ diffusion, reflected by the slightly decreased Li-FSI coordination number as seen in Figure S3.

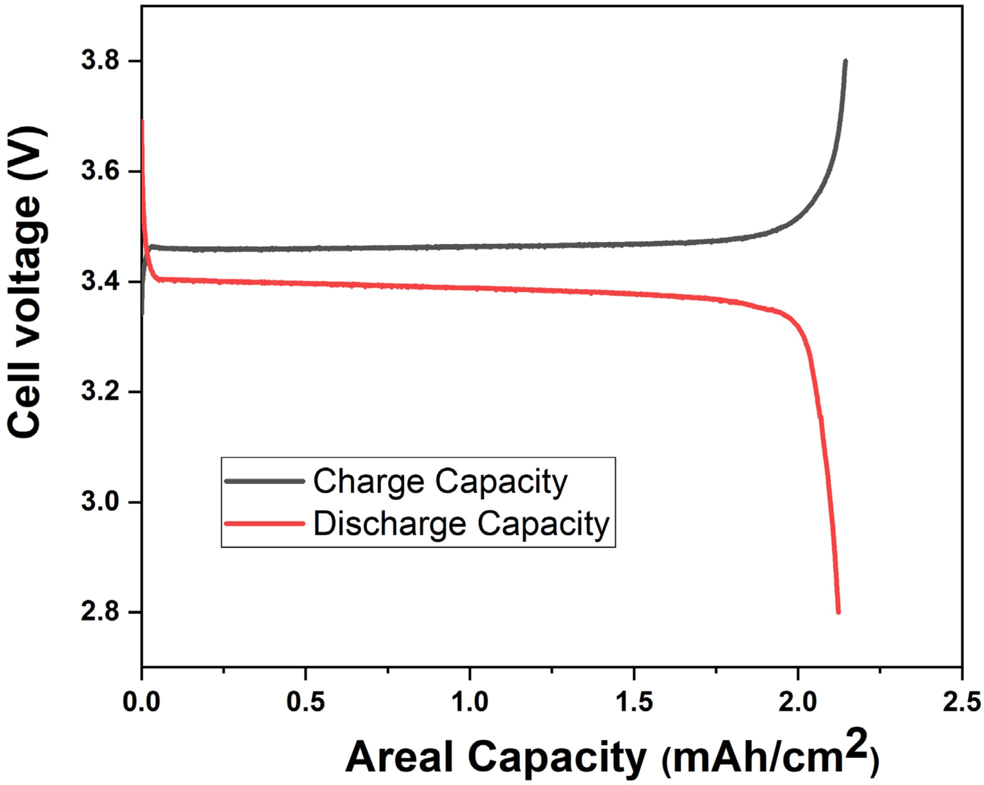

Figure S4: The one formation cycle at C/10 of the LFP/Li cell with 80IL20DME electrolyte using 2 mAh/cm^2 areal capacity cathode.

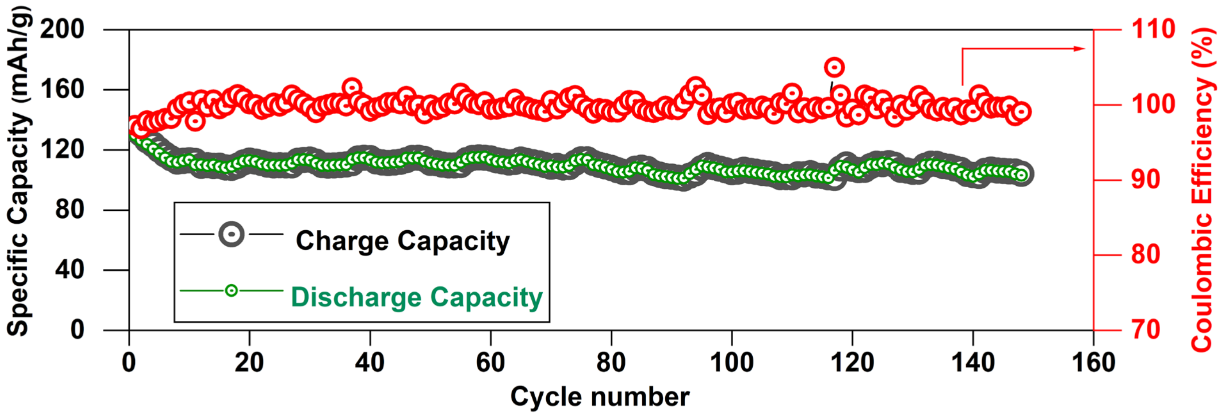

Figure S5: Galvanostatic room temperature cycling of LFP/Li cell at C/2 with 80IL20DME electrolyte using ~12 mg/cm^2 mass loading which corresponds to 2 mAh/cm^2 capacity.

The long term cycling of LFP/Li cell was also performed at room temperature (which is ~ 20 °C). Due to the higher viscosity of the 80IL20DME electrolyte at 20 °C (91 mPaS) than 50 °C

(30 mPaS), a lower specific capacity of ~120 mAh/g is obtained due to more difficult electrode wetting.

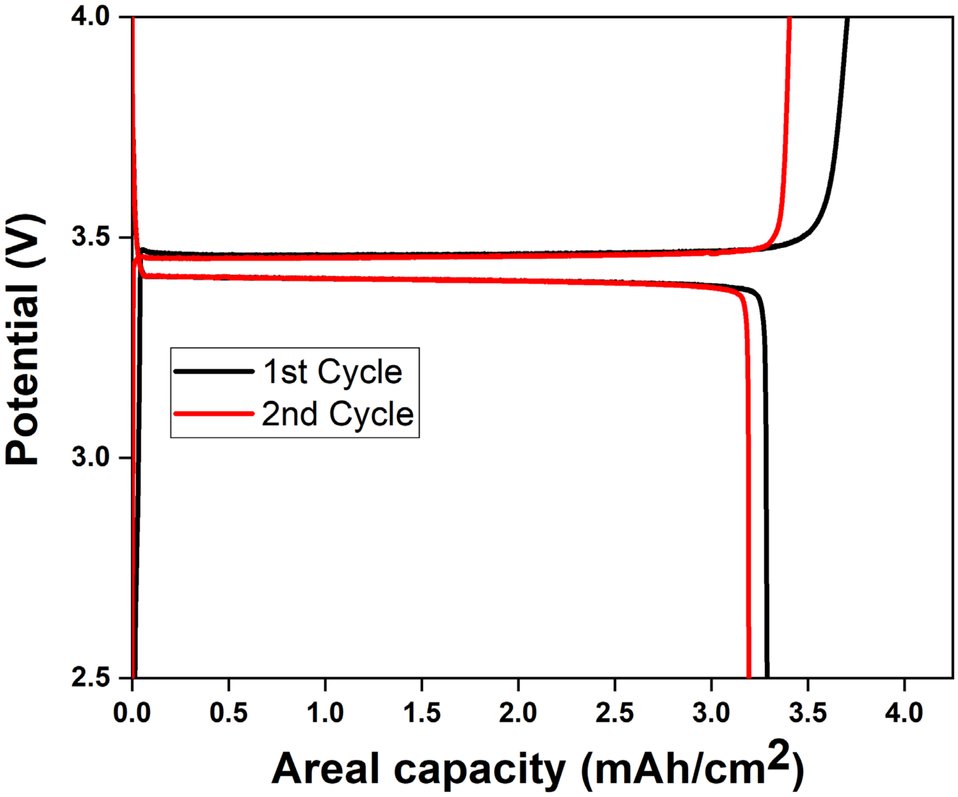

Figure S6: The two formation cycles at C/20 of the LFP/Cu cell with 80IL20DME electrolyte using 3.5 mAh/cm^2 areal capacity cathode.

The first cycle is considered to be very important in anode free cells as this step ensures the ability to plate the maximum capacity in that configuration. The LFP cathode used in this study had an areal capacity of 3.5 mAh/cm^2. During this experiment, we have applied very low current density (0.175 mA/cm^2) which corresponds to C/20 and we achieved a first cycle plating capacity of 3.7 mAh/cm^2, which is within the error of ~5% for electrode loading from the manufacturer. The first cycle Coulombic efficiency of 89% is very promising when compared to reported values in literature to date.

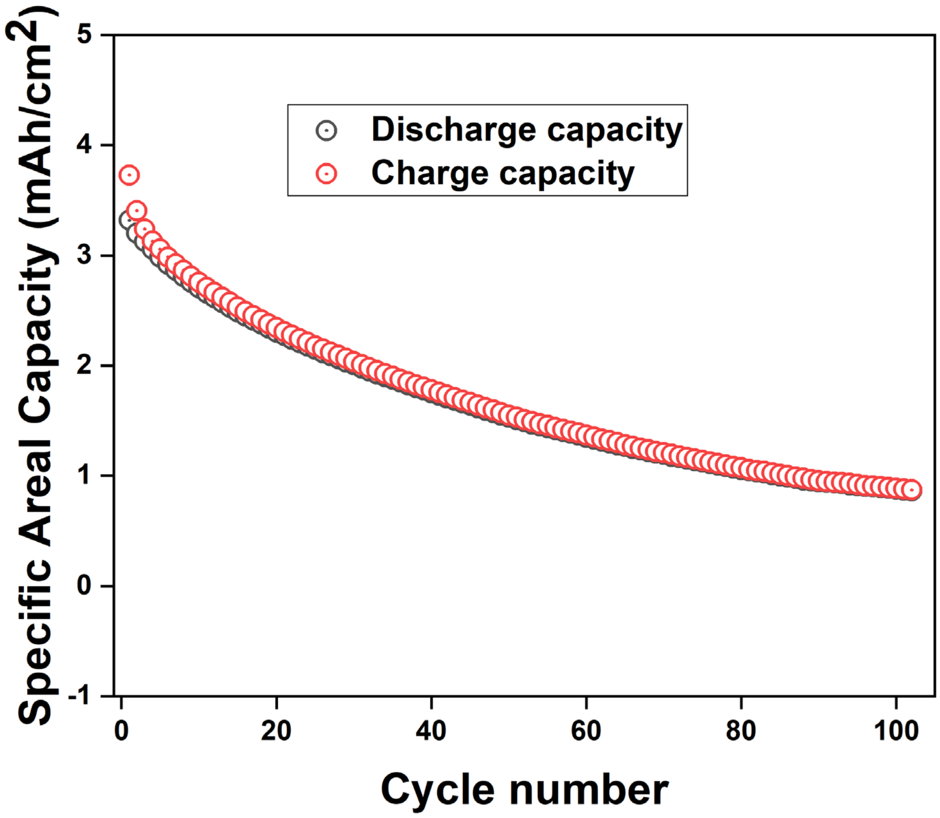

Figure S7: Long term galvanostatic cycling of anode free LFP/Cu cell with 80IL20DME electrolyte with 3.5 mAh/cm^2 areal cathode capacity.

Cycling to 100 cycles at C/2 (1.75 mA/cm^2) is shown here in Figure S6.

Table S3: Comparison of different electrolyte performance in LFP-Cu cells where the cathode areal capacities, applied current densities and LIRR value are compared.

Electrolyte	Cathode areal capacities	Current density	LIRR
4 M LiFSI in DME	1.6 mAh/cm^2	2 mA/cm^2	98.43%
1.86 M LiTFSI in EC	3.5 mAh/cm^2	1 mA/cm^2	97.07%
3.2 m LiFSI in 80IL20DME (our electrolyte)	3.5 mAh/cm^2	1.75 mA/cm^2	98.69% (with formation cycle) 98.72% (without formation cycle)